Biomacromolecules

pubs.acs.org/Biomac

Article

Antioxidant and UV-Blocking Leather-Inspired Nanocellulose-Based Films with High Wet Strength

Konstantin Kriechbaum and Lennart Bergström*

Cite This: *Biomacromolecules* 2020, 21, 1720–1728

Read Online

ACCESS | Metrics & More | Article Recommendations | Supporting Information

ABSTRACT: The mechanical performance in the wet state needs to be significantly improved and the intrinsic functionalities should be fully utilized to promote the replacement of fossil-based plastics with renewable biobased materials. We demonstrate a leather-inspired approach to produce multifunctional materials with a high wet strength that is based on tannin-induced precipitation of gelatin grafted onto surface-modified cellulose nanofibrils (CNF). The leather-inspired CNF-based films had a wet tensile strength of 33 MPa, a Young's modulus of 310 MPa, and a strain at failure of 22%, making the wet materials stronger than, for example, dry conventional low-density polyethylene and more ductile than paper-based food packaging materials. The tannin-containing films displayed excellent antioxidant and UV-blocking properties, rapidly scavenging more than 90% of added free radicals and absorbing 100% of light in the UV-B/UV-C range. This work illustrates the prospect of combining renewable materials in a leather-inspired approach to form wet strong and multifunctional films with potential application in food packaging.

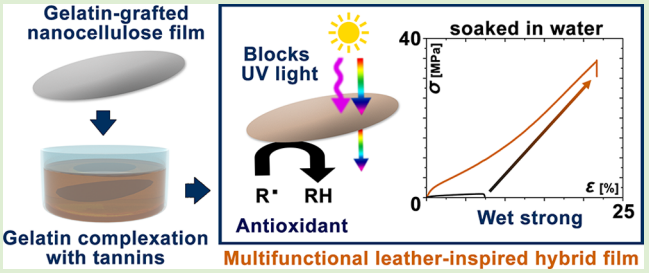

INTRODUCTION

Renewable and biodegradable alternatives to fossil-based and nonbiodegradable packaging materials are needed. Commercially available biodegradable plastics from renewable sources used for packaging include, for example, polylactic acid and polyhydroxyalkonates and chemically modified natural products, for example, cellulose, starch, or chitin.[1] Cellulose, the most abundant biopolymer on Earth, is an important raw material for industrial scale production of sustainable materials.[2] Nanocellulose, which can be extracted from cellulose by well-established processes,[3] has attracted substantial attention due its low density, high mechanical strength, and chemical inertness[4] and nanocellulose-based materials are being considered in food packaging applications to minimize the carbon footprint and reduce the weight.[5] However, nanocellulose-based materials are substantially weakened when hydrated[6] and there is a need to develop multifunctional materials with a high strength and ductility in humid and wet conditions.[7]

There have been several attempts to improve the wet mechanical performance of materials based on cellulose nanofibrils (CNF). The formation of covalent bonds between chemically modified CNF has yielded films with significantly increased wet strength and ductility compared to nonmodified CNF films, but with increased brittleness at dry conditions.[8,9] Nanocomposites with covalent ester cross-links between CNF and poly(acrylic acid),[10] polyamide epichlorohydrin resin,[11] vitrimer nanoparticles,[12] or PEG-maleimide[13] have better wet and dry strength than non-cross-linked CNF films, but rely on the use of fossil-based components. Hot-pressing mixtures of CNF and lignocellulosic wood nanofibers[14] and vacuum filtration of lignin-containing CNF from tobacco stalk[15] yielded materials with better wet mechanical properties than lignin-free CNF films, which in both studies was attributed to the ability of lignin to act as a barrier for water penetration. However, the dry mechanical properties of films from lignocellulosic wood nanofibers were impaired[14] and the fabrication of films from tobacco stalk CNF requires the use of organic solvents.[15] Cross-linking TEMPO-oxidized CNF using multivalent cations resulted in strong but brittle wet films (Fe^{3+} or Al^{3+}) or weak wet films with high strain at failure (Ca^{2+} and Mg^{2+}).[16] Films of mixtures of CNF and chitosan that had been treated with 0.1-M NaOH displayed tensile strengths as high as 100 MPa in the wet state, but the materials were strongly pH dependent and the strength was significantly reduced below pH 7.[17] Ionic cross-linking of tape-cast CNF/carboxymethyl cellulose composite films with glycidyl trimethylammonium chloride led to improved orientation-dependent mechanical properties both in the wet and dry states.[18] In two recent studies, Wågberg and co-workers showed that complexation of algal polysaccharides in interpenetrating networks with carboxymethylated CNF with Ca^{2+}

Special Issue: Anselme Payen Award Special Issue

Received: December 2, 2019
Revised: January 12, 2020
Published: January 16, 2020

https://dx.doi.org/10.1021/acs.biomac.9b01655
Biomacromolecules 2020, 21, 1720–1728

and Fe^{3+} resulted in films with tensile strengths of 17 and 40 MPa in the wet state, respectively.[19,20]

There is a growing trend toward active food packaging that incorporate, for example, antioxidant compounds to extend the shelf life of food products by protecting them against lipid oxidation, a main cause of food spoilage.[21] Synthetic polymers, such as polypyrrole,[22] or natural compounds like bromelain,[23] nisin,[24] berry polyphenols,[25] and curcumin,[26] have been used to confer nanocellulose-based materials with antioxidant properties. Recent work on nanocellulose-based materials incorporating tannins, which are astringent polyphenolic compounds that occur in the bark and leaves of many plants, resulted in films with increased antioxidant and UV-absorbing properties.[27,28]

Although CNF/tannin composites have promising functional properties and can further be patterned by forming colored complexes with metal ions,[29] they cannot be practically implemented in packaging without improved wet mechanical strength. In this study, we have exploited the ability of tannins to form insoluble complexes with proteins, which is the basis of leather tanning[30] that converts the putrescible skin into a material that is resistant to microbial attack and remains strong and flexible during uptake and release of moisture.[31]

Wet-stable multifunctional films were prepared from CNF and tannins derived from trees and gelatin obtained from bovine skin collagen using a leather-inspired approach where gelatin was covalently grafted on dialdehyde-functionalized CNF and physically cross-linked by the formation of insoluble complexes with tannins. The antioxidant and UV-blocking leather-inspired hybrid films had wet mechanical properties that are comparable to the dry strength of fossil-based polymer films, such as low-density polyethylene packaging, and low water uptake while retaining most of the exceptional dry mechanical properties of CNF-based films.

EXPERIMENTAL SECTION

Materials. Never-dried bleached Kraft softwood pulp was kindly provided by SCA Östrand (Sweden). The pulp was treated with 0.5 M HCl(aq), ion-exchanged to sodium form using 10^{-3} M $NaHCO_3$(aq), and washed thoroughly until neutral pH with deionized water. Tannic acid (TA, Alfa Aesar), gelatin from bovine skin (Type B, Sigma-Aldrich), $NaIO_4$ (≥99.8%, Sigma-Aldrich), sodium dodecyl sulfate (SDS, ≥99%, Sigma-Aldrich), triethanolamine (TEA, ≥99%, Merck Chemicals), NaCl (≥99.5%, Scharlau Chemicals), $NaHCO_3$ (≥99.5%, Sigma-Aldrich), $NH_2OH{\cdot}HCl$ (≥99%, Sigma-Aldrich), NaOH (≥99.2%, VWR Chemicals), and HCl(aq) (35%, VWR Chemicals) were used as received.

Preparation of CNF. A 2 wt % suspension of washed pulp fibers in deionized water was dispersed for 5 min using a High-Shear Dispermix (Ystral GmbH, Germany) and passed through a supermasscolloider grinder (model MKZA10-15J, Masuko Sangyo Co. Ltd., Japan, disk model MKE 10-46#) for mechanical fibrillation to give CNF as reported.[32]

Preparation of DACNF. CNF were oxidized to dialdehyde CNF (DACNF) by slowly adding 2.5 g $NaIO_4$ to 500 mL of a 0.5 wt % CNF suspension in deionized water (weight $NaIO_4$:CNF = 1:1) and subsequently stirring in a beaker for 4 h at room temperature. The beaker was wrapped in aluminum foil to prevent light-induced decomposition of periodate and undesired side reactions.[33] The DACNF suspension was filtered and washed with deionized water until the conductivity of the filtrate was <5 μS cm^{-1}. The final DACNF suspension was transferred to a glass bottle and stored at 4 °C until use.

Determination of Aldehyde Content. The amount of aldehyde groups introduced by periodate oxidation of CNF was determined by reaction with hydroxylamine hydrochloride, during which the formation of oximes releases stoichiometric amounts of protons.[34] A certain amount of DACNF suspension of known concentration was weighed in and acidified to pH 4 with 0.1 M HCl(aq). A total of 25 mL of 0.25 M $NH_2OH{\cdot}HCl$(aq), adjusted to pH 4 with NaOH(aq), was added, and the mixture was stirred for 2 h before being titrated back to pH 4 using 0.1 M NaOH(aq). The amount of aldehyde groups per sample weight was calculated from the moles of NaOH consumed. A degree of oxidation was calculated considering a maximum value of 12.34 mmol g^{-1} for completely oxidized CNF, as each anhydrous glucose unit of the cellulose polymer could yield two aldehyde groups. The oxime formation and subsequent titration were performed three separate times for each material.

Grafting of Gelatin to DACNF To Form Gelatin@DACNF. Gelatin (type B, isoelectric point = 4.7−5.3, 250 mg) was added to 250 mL of a 0.3 wt % DACNF suspension that had been preheated to 60 °C in a round-bottom flask (weight DACNF:gelatin = 3:1). The pH of the suspension was raised to 6.5 by adding 0.1 M NaOH and the mixture was stirred at 60 °C for 3 h. The resulting suspension was allowed to cool down and used immediately.

Determination of the Degree of Modification. The coupling between DACNF and gelatin was demonstrated in several ways. The amount of aldehyde groups per dry sample weight was measured both for the Gelatin@DACNF suspension and for a gelatin reference via reaction with $NH_2OH{\cdot}HCl$ and subsequent titration with NaOH (see above). The consumption of aldehydes was calculated according to eq 1.

$$\text{aldehyde consumption}[\%] = \left\{1 - \frac{\text{aldehydes}_{\text{gelatin@DACNF}} - \text{aldehydes}_{\text{gelatin}}}{\text{aldehydes}_{\text{DACNF}}}\right\} \times 100 \quad (1)$$

Tollens' reagent was used to visualize the decrease in surface aldehyde groups on CNF. A total of 0.5 mL of Tollens' reagent were added to 100 mg each of a CNF reference and the DACNF and Gelatin@DACNF suspensions, and shaken for 5 min. The suspensions were centrifuged and the pellets were washed three times with deionized water, dried, and examined using a JEOL JSM-7401F (JEOL Ltd., Japan) scanning electron microscope. Images were recorded at an accelerating voltage of 2 kV and a working distance of 8 mm.

The decrease in gelatin primary amino groups upon coupling to DACNF was determined by a modified ninhydrin (2,2-dihydroxyindane-1,3-dione) assay.[35] A total of 1 mL of ninhydrin solution (1.5% in ethanol, w/v) was added to a dry film sample in a test tube and heated to 80 °C for 45 min. The suspension was allowed to cool to room temperature and diluted with deionized water before its absorbance at 570 nm was measured on a Lambda 19 UV/Vis spectrometer (PerkinElmer, U.S.A.) against deionized water containing the same amount of ninhydrin. The amount of free amino groups in gelatin before and after coupling is proportional to the optical absorbance of the solution.[36]

Preparation of Films. Films of CNF, DACNF, and Gelatin@DACNF were produced by vacuum filtration and subsequent drying. Therefore, 15 g of 0.3 wt % suspensions were filtered through nylon membranes (GVS, 0.45 μm, hydrophilic) by applying a vacuum. The resulting wet cake was rinsed with 10 mL of deionized water to remove nonbound gelatin. Films were formed by drying the wet cake between sheets of paper overnight at room temperature under a weight.

Tanning of Films To Form TA/Gelatin@DACNF. Dry CNF/Gelatin and Gelatin@DACNF films were immersed in 10 mg mL^{-1} TA solutions for 24 h at 23 °C, then rinsed with copious amounts of deionized water, and immersed in deionized water for 2 h before being dried according to the procedure above.

Characterization of Films. The amount of gelatin and tannin in the hybrid films was determined gravimetrically by comparing the weight of at least three dry films before and after modification.

The mechanical properties of the films in the wet and dry state were measured using an Instron 5966 universal testing machine (Instron, U.S.A.) equipped with a 100 N load cell at a strain rate of 1

https://dx.doi.org/10.1021/acs.biomac.9b01655
Biomacromolecules 2020, 21, 1720−1728

mm min^{-1}. The mechanical measurements were performed on films with a rectangular shape and dimensions of 20 × 3 mm using a gauge length of 10 mm. The dry films were conditioned at 50% RH and 23 °C at least 24 h prior to measurement and their thickness was measured using a digimatic micrometer (Mitutoyo, Japan, accuracy 0.1 μm). The wet mechanical properties were determined on films that had been immersed in deionized water or aqueous solutions of simulated seawater (pH 8.2, 3.5 wt % NaCl in tap water) or TEA/SDS (5% v/v TEA + 1% w/v SDS in deionized water) for 1 h before measurement. The wet thickness of the films was calculated by multiplying their dry thicknesses with a swelling ratio that was determined from optical microscopy images of the cross sections of at least four films before and after immersion for 1 h (Table S1). To ensure that the wet films are fully saturated during the measurements, a drop of deionized water was placed on the bottom clamp, covering parts of the film during testing. The Young's modulus was calculated from the slope of the linear part of the stress−strain curve. Toughness was determined from the area under the stress−strain curve up to the point of fracture. The average data for each material is reported based on 4−10 films and the combined standard uncertainty is calculated as the root sum of the squares of relative standard deviations of the measurement and the film thickness.

The water uptake of the films was determined by measuring their weight before and after immersion in deionized water for 1 h. The weight of the wet sample was determined on an analytical balance after blotting the excess water with dry filter paper. The water uptake is expressed as the percentage weight increase compared to the initial dry mass, based on measurements of three films.

The cross-sectional structure of swollen films was characterized by scanning electron microscopy after immersing the films in deionized water for 1 h and subsequent crash freezing, cryo-fracturing, and freeze-drying. Scanning electron microscopy images were recorded on a JEOL JSM-7401F (JEOL Ltd., Japan) after coating the swollen and freeze-dried films with a thin layer of gold, using an accelerating voltage of 2 kV and a working distance of 8 mm.

Infrared spectra of dried films were measured on a Varian 670-IR FTIR spectrometer (Varian, U.S.A.), equipped with an attenuated total reflection detection device with a single reflection diamond element. A total of 32 scans were accumulated with a spectral resolution of 4 cm^{-1}.

Thermal gravimetric analysis was performed on a Discovery TG (TA Instruments, U.S.A.), using a 40 mL min^{-1} nitrogen flow and a heating rate of 10 °C min^{-1}.

The optical properties of films were investigated by measuring their in-line transmittance with a Genesys 150 UV−visible spectrometer (Thermo Fisher Scientific, U.S.A.) in the range of 200−800 nm using air as background. Measurements were performed on three films for each material.

The antioxidant activity of films was determined by the 2,2-diphenyl-1-picrylhydrazyl (DPPH) radical scavenging method.[37] A total of 10 mg of the films was immersed in 1 mL of 0.1 mM DPPH in methanol. The mixtures were vortexed and left in the dark at room temperature. Absorbance values at 517 nm were measured on a Lambda 19 UV/Vis spectrometer (PerkinElmer, U.S.A.) after 5 min and 5 h. DPPH radical scavenging activity was calculated by eq 2, where A_s is the absorbance of the supernatant solution after reaction with the film and A_{ref} is the absorbance of 0.1 mM DPPH in methanol. The average of two measurements per sample is reported.

$$\text{DPPH inhibition}[\%] = \left(\frac{A_{ref} - A_s}{A_{ref}}\right) \times 100 \quad (2)$$

RESULTS AND DISCUSSION

Preparation of Films. We have used a leather-inspired approach based on tannin-induced precipitation of gelatin to prepare CNF-based films. Gelatin, a widely abundant protein, was grafted onto dialdehyde-modified CNF (DACNF) with an aldehyde content of 0.74 ± 0.02 mmol g^{-1} (6% of anhydroglucose units oxidized). The Gelatin@DACNF was dispersed in water (Figure 1a) and self-standing films were prepared by vacuum filtration (Figure 1b). The vacuum-filtrated films, including Gelatin@DACNF films (Figure 1c), were submerged in an aqueous solution of tannic acid (Figure 1d). Tannin treatment of Gelatin@DACNF films resulted in translucent leather-inspired TA/Gelatin@DACNF hybrid films with a slight brown coloration (Figure 1e) where the grafted gelatin is complexed by tannin (Figure 1f).

The grafting of gelatin on DACNF between DACNF aldehydes and the gelatin amine groups was performed via a Maillard-type reaction[38] at pH 6.5 to avoid depolymerization of DACNF that can occur at alkaline conditions.[39] Grafting the gelatin onto CNF resulted in a gelatin content of 5.9 wt % in the vacuum filtrated Gelatin@DACNF film, which is significantly higher compared to the gelatin content of 3.7 wt % in vacuum filtrated films of gelatin and CNF mixtures (CNF/Gelatin; Table 1). The aldehyde content of DACNF, as measured by titration with hydroxylamine hydrochloride, decreased from 0.78 to 0.55 mmol g^{-1} after grafting of gelatin. Increasing the time for the grafting reaction did not result in a further decrease of the aldehyde content, which suggests that the remaining, not already reacted, aldehyde groups were inaccessible to react with gelatin. This indicates that a fraction of the aldehyde groups are located inside the fibril, which is supported by a recent study on periodate oxidation of nanocellulose that was shown to occur not only on the fibril surface, but also inside the fibrils.[40] Figure 2a shows that the coverage of the bright silver nanoparticles was significantly lower when diamminesilver(I) (Tollens' reagent) was applied to Gelatin@DACNF compared to DACNF films, which supports that the density of aldehyde groups (that can participate in redox reactions) was reduced by the gelatin grafting reaction. Infrared spectroscopy provides further support for a successful grafting reaction, as the characteristic band for the aldehyde carbonyls at 1740 cm^{-1} was absent in the IR spectrum of the Gelatin@DACNF films, whereas amide bands of gelatin appeared at 1637, 1525, and 1259 cm^{-1}, respectively (Figure 2b). The reduction of primary amine groups in gelatin that was grafted to DACNF (Gelatin@DACNF films) compared to gelatin that was only mixed but not grafted to CNF (CNF/Gelatin films) was confirmed with a modified ninhydrin colorimetric assay. Primary amines form purple chromophores on reaction with ninhydrin and comparing the absorbance at 570 nm of equal amounts of grafted and added gelatin with an UV/Vis spectrometer can be used to calculate the degree of gelatin cross-linking (eq 3), where $A_{Gelatin@DACNF}$ and $A_{CNF/Gelatin}$ are measured for samples containing the same amount of gelatin.

$$\text{degree of gelatin cross-linking}[\%] = \left\{1 - \frac{A_{gelatin@DACNF}}{A_{CNF/gelatin}}\right\} \times 100 \quad (3)$$

The average absorbance at 570 nm decreased from 0.042 (CNF/Gelatin) to 0.018 (Gelatin@DACNF) resulting in a cross-linking degree of 57%, which suggests that more than half of the gelatin primary amines reacted during grafting with DACNF.

Leather-Inspired Tanning of Films. The Gelatin@DACNF films were submerged in an aqueous solution of tannic acid to cross-link the gelatin in a leather-inspired process. The IR spectrum of the TA/Gelatin@DACNF film featured characteristic bands for tannic acid carbonyl groups at

https://dx.doi.org/10.1021/acs.biomac.9b01655
Biomacromolecules 2020, 21, 1720−1728

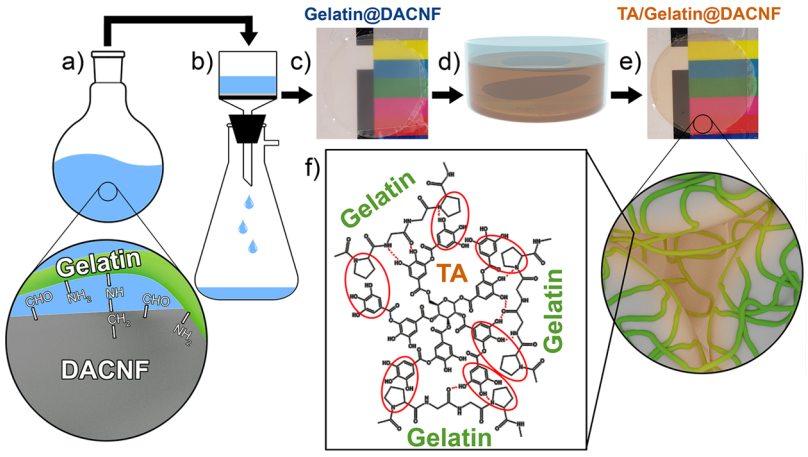

Figure 1. Processing of TA/Gelatin@DACNF films: (a) grafting of gelatin on DACNF; (b) vacuum filtration of an aqueous dispersion of the components; (c) transparent Gelatin@DACNF film; (d) subjecting the vacuum filtrated film to an aqueous solution of tannic acid; (e) slightly brownish TA/Gelatin@DACNF film; (f) schematic illustration of the complexation of gelatin with tannic acid.

Table 1. Composition and Thickness of CNF- or DACNF-Based Hybrid Films

		Composition		
Material	Thickness [μm]	CNF/DACNF [wt%]	Gelatin [wt%]	Tannin [wt%]
CNF	40.8 ± 1.4	100		
CNF/Gelatin	43.9 ± 1.0	96.3 ± 2.3	3.7 ± 2.3	
CNF/Gelatin/TA	45.7 ± 1.7	91.1 ± 4.1	3.5 ± 2.2	5.5 ± 3.9
DACNF	50.8 ± 1.5	100		
Gelatin@DACNF	53.8 ± 1.4	94.1 ± 0.7	5.9 ± 0.8	
TA/Gelatin@DACNF	54.2 ± 1.3	83.5 ± 0.5	5.2 ± 0.7	11.2 ± 0.4

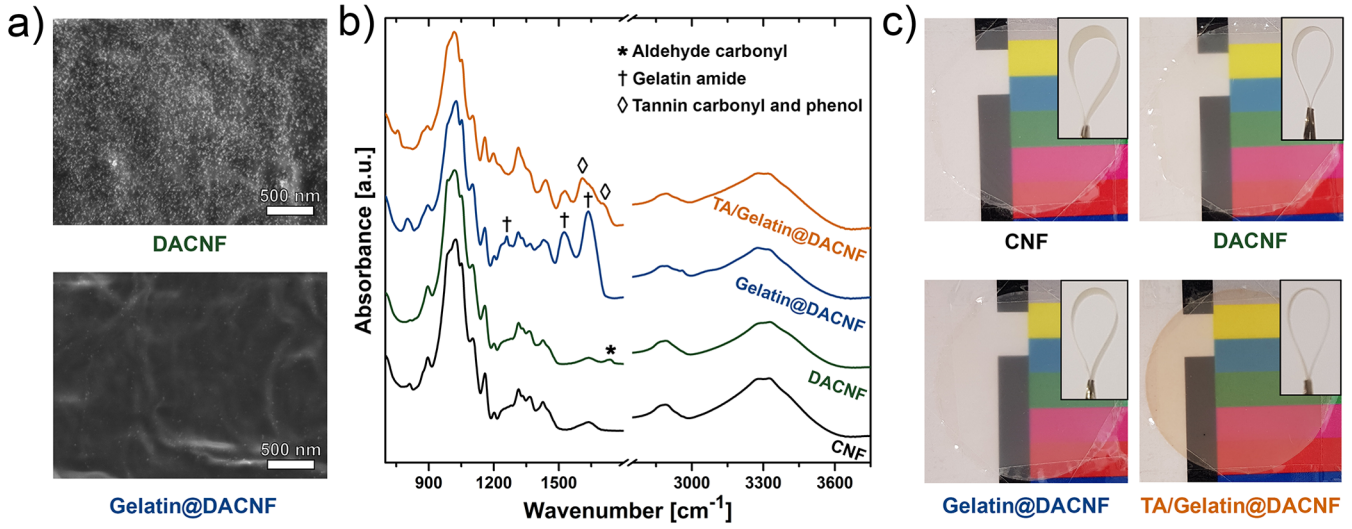

Figure 2. Characterization of the hybrid CNF-based films: (a) SEM pictures of DACNF and Gelatin@DACNF after reaction with diamminesilver(I) (Tollens' reagent); (b) IR spectra; and (c) images of CNF, DACNF, Gelatin@DACNF, and TA/Gelatin@DACNF films.

1700 cm^{-1} and phenolic groups at 1608 cm^{-1} (Figure 2b). The hybrid TA/Gelatin@DACNF films were translucent, with a slight brown coloration after tanning (Figure 2c). The main degradation step in N_2 of Gelatin@DACNF films complexed with tannin started at a lower temperature, was less intense, and yielded a higher fraction of residual material compared to the noncomplexed Gelatin@DACNF film (Figure S1). The final residue of TA/Gelatin@DACNF films (32 wt % residue) significantly exceeds the estimated contribution of the residues from each of the components (24 wt % residue), which suggests that TA complexation promotes char formation. The TA-related decrease in degradation temperature and increase in char yield are in good agreement with previous work on the thermal degradation of cellulose that has been treated with tannin.[41]

Previous work has shown that gelatin is precipitated by the tannic acid molecules and form insoluble complexes via hydrogen bonding and hydrophobic interactions.[42] The neat CNF film immersed in a tannic acid solution retained on average 3.7 wt % tannin after washing, which suggests that

https://dx.doi.org/10.1021/acs.biomac.9b01655
Biomacromolecules 2020, 21, 1720−1728

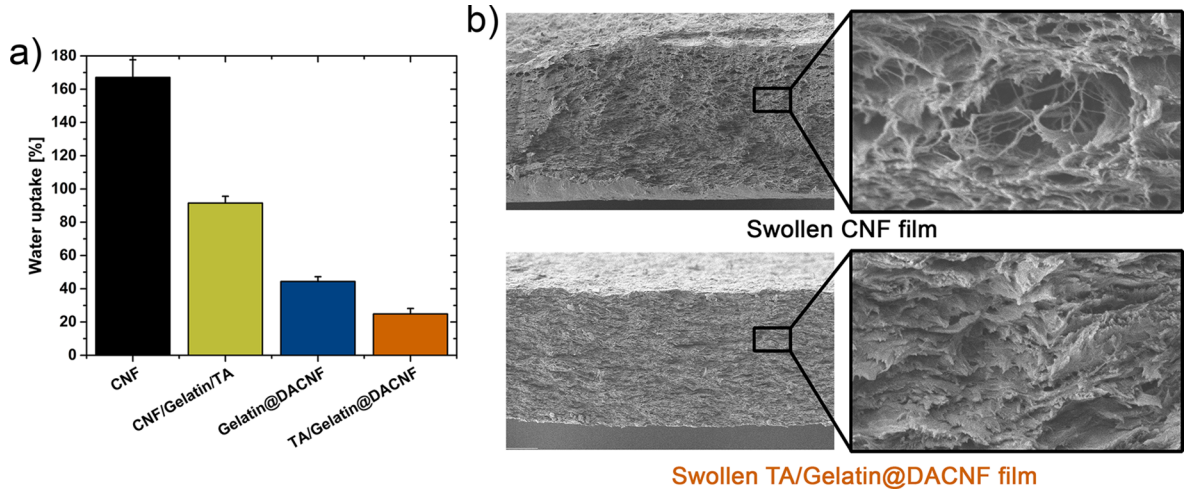

Figure 3. Water uptake and swelling of CNF-based films: (a) Water uptake of CNF-based films. Scanning electron microscopy images of swollen and freeze-dried film cross sections of (b) neat CNF films and leather-inspired TA/Gelatin@DACNF hybrid films.

Table 2. Tensile Mechanical Properties of Wet and Dry CNF-Based Films

	Strain at failure		Tensile strength		Young's modulus		Toughness	
Sample	Dry [%]	Wet [%]	Dry [MPa]	Wet [MPa]	Dry [GPa]	Wet [MPa]	Dry [MJ m^{-3}]	Wet [MJ m^{-3}]
CNF	15.5 ± 2.5	6.7 ± 1.0	139 ± 9	0.9 ± 0.1	4.4 ± 0.3	26 ± 4	16.1 ± 2.7	0.04 ± 0.00
CNF/Gelatin	11.9 ± 1.4	7.2 ± 0.8	134 ± 7	0.9 ± 0.1	4.5 ± 0.2	22 ± 3	12.0 ± 1.8	0.04 ± 0.01
CNF/Gelatin/TA	12.8 ± 1.6	11.8 ± 1.2	148 ± 12	3.1 ± 0.4	4.8 ± 0.2	73 ± 8	14.8 ± 2.8	0.22 ± 0.03
DACNF	10.3 ± 2.4	16.5 ± 1.0	115 ± 11	9.9 ± 1.2	3.9 ± 0.2	138 ± 11	9.0 ± 3.0	0.88 ± 0.10
Gelatin@DACNF	12.0 ± 1.2	23.2 ± 2.2	118 ± 4	15.4 ± 1.3	4.4 ± 0.2	94 ± 6	11.1 ± 1.1	1.58 ± 0.22
TA/Gelatin@DACNF	11.4 ± 1.6	22.1 ± 2.3	140 ± 12	33.0 ± 2.3	4.7 ± 0.2	312 ± 26	12.6 ± 2.5	3.37 ± 0.36
TA/Gelatin@DACNF in simulated seawater		24.5 ± 2.0		28.8 ± 2.6		284 ± 11		3.26 ± 0.52
TA/Gelatin@DACNF in SDS/TEA (aq.)		23.3 ± 2.8		8.5 ± 1.1		73 ± 6		0.96 ± 0.21

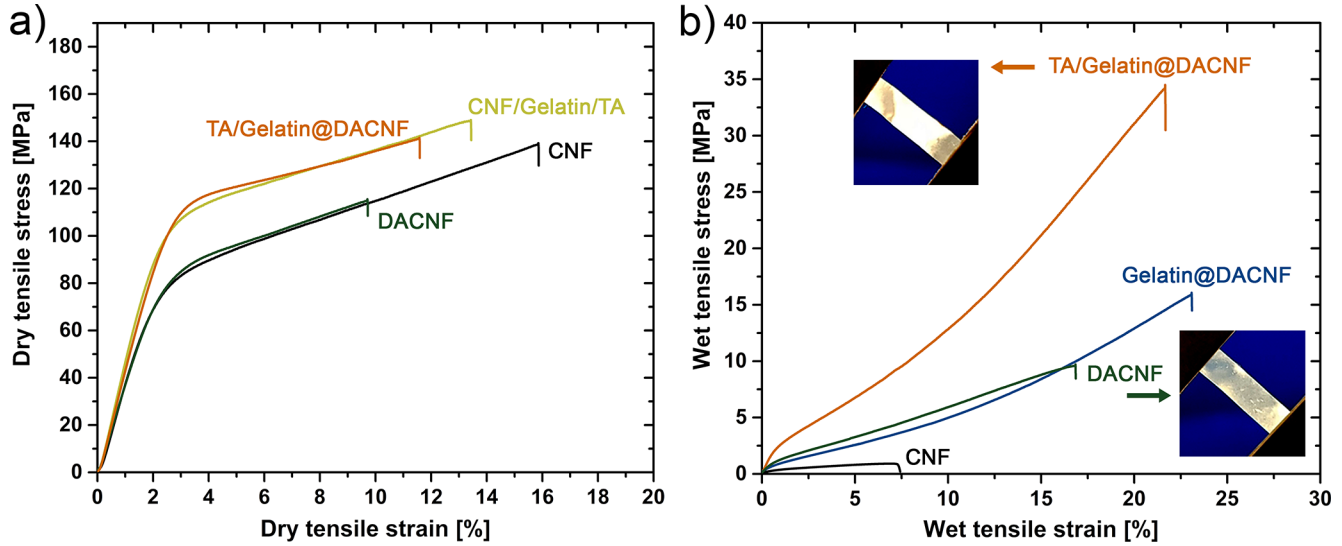

Figure 4. Representative stress−strain curves of CNF-based films in the (a) dry state and (b) wet state with (inset) digital images of film samples after tensile testing between crossed polarizers. The elongation direction is aligned 45° with respect to the crossed polarized planes.

tannic acid adsorbs onto cellulose.[43] However, three times more tannic acid was incorporated in the gelatin-containing TA/Gelatin@DACNF films (11.2 wt % TA) compared to the CNF films, which shows that tannic acid forms insoluble complexes with the grafted gelatin. Previous work has shown that gelatin and hydrolyzable tannin form complexes with a tannin/gelatin ratio of 3:2 at low gelatin concentrations,[44] which is in very good agreement with the tannin/gelatin ratio of 3.1:2 in our hybrid TA/Gelatin@DACNF films, assuming that the amount of adsorbed tannic acid is similar to Gelatin@DACNF and CNF.

https://dx.doi.org/10.1021/acs.biomac.9b01655
Biomacromolecules 2020, 21, 1720−1728

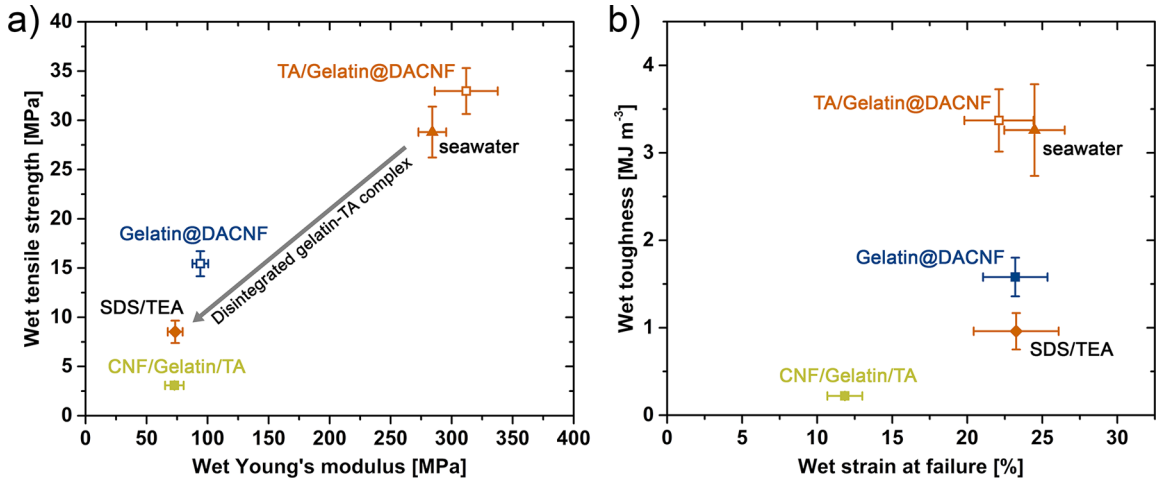

Figure 5. Ashby plots of the mechanical properties of CNF-based films in the wet state: (a) tensile strength vs Young's modulus and; (b) strain at failure vs toughness of tannic acid treated films of CNF/gelatin mixtures (CNF/Gelatin/TA), gelatin-grafted DACNF (Gelatin@DACNF) after immersion in deionized water, and the tanned gelatin-grafted DACNF film (TA/Gelatin@DACNF) after immersion in deionized water, simulated seawater, or an aqueous SDS/TEA solution.

Water Uptake and Swelling of CNF-Based Films. The water uptake of CNF and TA/Gelatin@DACNF films was assessed gravimetrically (Figure 3a), and freeze-dried water-containing films were also examined using SEM (Figure 3b). Figure 3a shows that soaking the leather-inspired TA/Gelatin@DACNF hybrid films in water for 1 h resulted in a weight increase of only 25%, while the neat CNF films increased their weight with 167%. The formation of water-insoluble complexes between the grafted gelatin and the added tannins resulted in a significantly smaller swelling of the TA/Gelatin@DACNF hybrid films compared to the neat CNF films that displayed an open and porous film structure with interconnected nanofibrils (Figure 3b). Soaking CNF/Gelatin films in water resulted in a similar water uptake as the neat CNF films (141% for CNF/Gelatin, cf. 167% for CNF), while tanning these films (CNF/Gelatin/TA) resulted in a water uptake of 92%, which is less than the CNF/Gelatin films, but much higher compared to the TA/Gelatin@DACNF hybrid films (Figure 3a). Films of neat DACNF had a relative water uptake of 40%, which suggests that the formation of interfibril hemiacetal linkages[45] results in a significant decrease of the water uptake compared to neat CNF films. The water uptake of films with gelatin grafted to DACNF (Gelatin@DACNF) was slightly higher (44%) compared to neat DACNF (40%), which probably is related to the reduction in aldehyde groups available to form interfibril hemiacetal linkages. In summary, the formation of a CNF-based material held together by insoluble grafted gelatin−tannin complexes (TA/Gelatin@DACNF) results in a lower water uptake (25% weight increase) compared to any of the other material combinations, for example, CNF/Gelatin/TA (92%) or Gelatin@DACNF films (44%).

Mechanical Properties in the Wet and Dry State. The mechanical properties of the CNF-based films have been evaluated by tensile testing in the dry state after conditioning at 50% relative humidity and 23 °C, and in the wet state on films retrieved after immersion for 1 h in water, in simulated seawater at pH 8.2, or in a sodium dodecyl sulfonate (SDS)/triethanol amine (TEA) solution (Table 2).

The CNF-based films measured in the dry state show an elastic behavior at low strains, which is followed by plastic deformation until the film finally breaks when the strain at failure is reached (Figure 4a). The Young's modulus of dry leather-inspired TA/Gelatin@DACNF hybrid films was slightly higher compared to neat CNF films, while the tensile strength was similar (Table 2). Films made from DACNF or Gelatin@DACNF, however, displayed a lower Young's modulus and tensile strength in the dry state compared to the leather-inspired hybrid films. Interestingly, complexation of gelatin with tannins in CNF films were gelatin was not grafted (CNF/Gelatin/TA) results in films with higher dry tensile strength and stiffness, which may be related to additional hydrogen bonds between the hydroxyproline-rich gelatin−tannin complexes and the CNF matrix.[46]

The wet films displayed only a small elastic region followed by a plastic region that extends up to strains exceeding 20% (Figure 4b). The gelatin-grafted Gelatin@DACNF hybrid films and the leather-inspired TA/Gelatin@DACNF hybrid films exhibited strain hardening, which in previous studies has been related to strain-induced fibril alignment.[47] Indeed, strain-induced fibril alignment of the TA/Gelatin@DACNF hybrid films was confirmed by observing the film between crossed polarizers after tensile testing. The TA/Gelatin@DACNF films displayed a high degree of birefringence with a maximum in light intensity at a 45° angle with respect to the crossed polarized planes. In comparison, the neat DACNF films showed a significantly smaller birefringence (Figure 4b, inset).

The leather-inspired TA/Gelatin@DACNF hybrid films displayed a tensile strength of 33 ± 2 MPa, Young's modulus of 312 ± 26 MPa, strain at failure of 22 ± 2%, and toughness of 3.4 ± 0.4 MJ m^{-3} in the wet state (Table 2). The mechanical properties of the wet TA/Gelatin@DACNF hybrid films are comparable or superior to the mechanical properties at dry conditions of biobased food packaging films,[48] commercial multilayer flexible plastic packaging,[49] commercial biodegradable poly(lactic-acid)-based films,[50] conventional LDPE packaging films,[51] or paper-based food packaging materials.[52] The high wet strength and Young's modulus of the TA/Gelatin@DACNF hybrid films is associated with strong but flexible interfibrillar cross-links,[19,20] which can be

https://dx.doi.org/10.1021/acs.biomac.9b01655
Biomacromolecules 2020, 21, 1720−1728

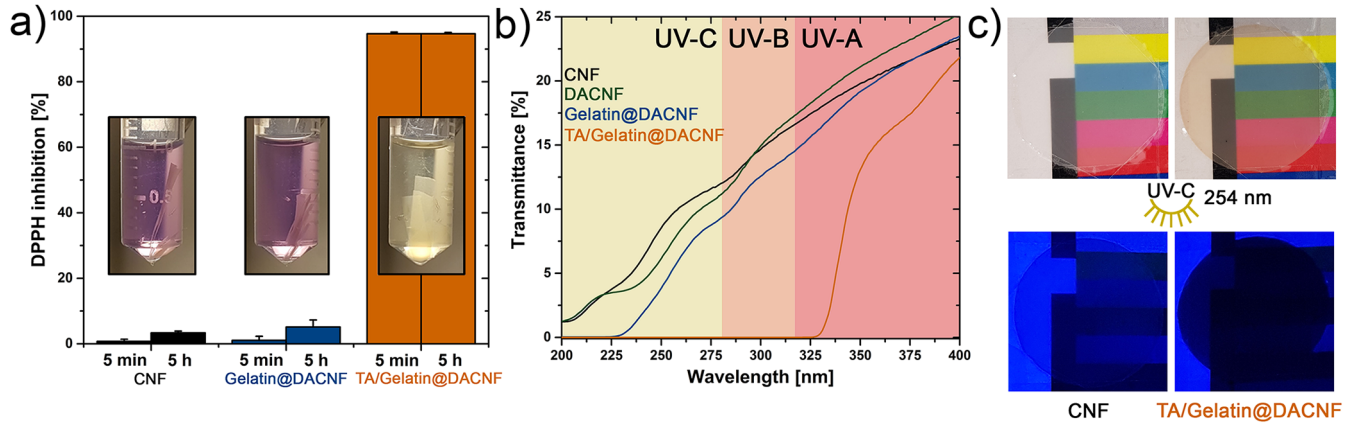

Figure 6. Antioxidant and optical properties of CNF-based films: (a) Antioxidant activity determined by DPPH inhibition after 5 min and 5 h, respectively, with insets showing images of the corresponding films in DPPH solutions. (b) Transmittance in the UV-A, UV-B, and UV-C range as a function of the wavelength. (c) Comparison of the UV-C absorbance of the nonmodified CNF film and the leather-inspired TA/Gelatin@DACNF hybrid film.

attributed to the insoluble complexes of the Gelatin@DACNF and TA.

Nonmodified CNF films became very weak after immersion in water, losing more than 99% of their dry tensile strength and Young's modulus, which correlates well with previous studies on CNF films.[18] Mixing CNF with gelatin (CNF/Gelatin) does not have any significant effect on the wet mechanical properties (Table 2). Complexing physically adsorbed gelatin with tannin resulted in a wet tensile strength and toughness of CNF/Gelatin/TA films that were about 3 and 6 times higher than neat CNF films, respectively. While the DACNF films display much higher wet mechanical properties than neat CNF films, we find that the wet tensile strength and toughness of the leather-inspired TA/Gelatin@DACNF hybrid films are over three times larger than the DACNF films and over two times higher compared to the Gelatin@DACNF films.

Figure 5 shows that soaking TA/Gelatin@DACNF films in an aqueous surfactant (SDS) and triethanolamine (TEA) solution disintegrates the gelatin-tannin complex[53] and results in a large decrease of both the wet strength, from 33 to 8.5 MPa, and stiffness, from 312 to 73 MPa (Table 2). The wet strength and stiffness after dissolution of the interfibrillar cross-links is comparable to physical mixtures of CNF and gelatin after tanning (CNF/Gelatin/TA) and lower than gelatin-grafted hybrid films before tanning (Gelatin@DACNF, Figure 5a). However, the relatively high wet strain at failure of the leather-inspired films after SDS/TEA treatment is similar to the Gelatin@DACNF films and much higher than the CNF/Gelatin/TA films (Figure 5b), which suggests that the grafting of the gelatin onto CNF was not affected by the SDS/TEA treatment.

The relatively small decrease of the wet mechanical properties of films immersed in simulated seawater (Figure 5) compared to films that had been immersed in deionized water (Table 2) shows that the tannin-complexed films are able to withstand high ionic strengths. The representative stress–strain curves of the leather-inspired films measured after soaking in SDS/TEA solution and simulated seawater are presented in Figure S2.

Antioxidant and UV-Blocking Properties of TA/Gelatin@DACNF films. The TA/Gelatin@DACNF film, which contained 11.2 wt % tannin, scavenged more than 94% of the 1,1-diphenyl-2-picrylhydrazyl (DPPH) radical after only 5 min, while the CNF and Gelatin@DACNF films displayed almost no reduction of the radicals even after 5 h (Figure 6a). In comparison, it was previously shown that composites of cationic-CNF and 10 wt % tannin scavenged around 31% of DPPH radicals after 30 min.[28] Hence, it is interesting to note that the leather-inspired films presented here trap radicals more efficiently compared to the tannin-containing cationic CNF-based films,[28] at similar tannin concentrations. In addition to scavenging free radicals, tannins have been shown to inhibit bacteria growth,[54,55] which suggests that incorporation of TA in CNF-based films could provide the materials with both antioxidant and antimicrobial properties.

Figure 6b shows that the tannin-containing TA/Gelatin@DACNF hybrid film with a thickness of around 50 μm blocked 100% of light in the UV-B/UV-C (200–315 nm) and on average 88% in the UV-A (315–400 nm) range, which is in good agreement with previous studies on tannin-containing nanocellulose films.[28] The π-conjugated system of tannins is rich in phenolic groups and efficiently absorbs light in the UV range, offering natural protection against solar radiation in plants.[56] The Gelatin@DACNF, DACNF, and CNF films that did not contain tannin transmitted on average between 20 and 22% of UV-A, 12 and 14% of UV-B, and 3 and 6% of UV-C light, respectively. Figure 6c shows that the tannin-containing hybrid film is opaque and blocks 254 nm UV-C light, while the nonmodified CNF reference film was translucent. Interestingly, the transmittance of visible light was not significantly affected by the introduction of tannin and was around 30% for all films (Figure S3). The antioxidant and UV-blocking capabilities of the leather-inspired hybrid films provide the wet strong materials with multifunctional properties that may be of interest for specific packaging applications.

CONCLUSION

Inspired by the tanning of leather, we have developed a route to physically cross-link CNF by the addition of tannic acid to hybrid films of gelatin-grafted cellulose nanofibers. The formation of water-insoluble tannin–gelatin complexes provided the leather-inspired TA/Gelatin@DACNF films with a high strength (33 MPa) and ductility (over 22% maximum strain) in the wet state, while retaining the attractive dry mechanical properties of neat CNF films (140 MPa strength

https://dx.doi.org/10.1021/acs.biomac.9b01655
Biomacromolecules 2020, 21, 1720–1728

and over 11% maximum strain). The polyphenolic tannin in TA/Gelatin@DACNF films effectively scavenged added free radicals (90% reduction after 5 min) and rendered the material opaque to UV-B/UV-C light, thus, conferring the films with antioxidant and UV-blocking properties. The leather-inspired approach to form wet strong and multifunctional CNF-based films from renewable components is of interest in food packaging and for biomedical applications.

■ ASSOCIATED CONTENT

Supporting Information

The Supporting Information is available free of charge at https://pubs.acs.org/doi/10.1021/acs.biomac.9b01655.

Additional information on the wet thickness, thermal stability, and transmittance in the visible spectrum of films and supplementary representative stress−strain curves (PDF)

■ AUTHOR INFORMATION

Corresponding Author

Lennart Bergström − *Department of Materials and Environmental Chemistry, Stockholm University 106 91 Stockholm, Sweden;* orcid.org/0000-0002-5702-0681; Email: lennart.bergstrom@mmk.su.se

Author

Konstantin Kriechbaum − *Department of Materials and Environmental Chemistry, Stockholm University 106 91 Stockholm, Sweden;* orcid.org/0000-0002-3737-5303

Complete contact information is available at: https://pubs.acs.org/10.1021/acs.biomac.9b01655

Author Contributions

The manuscript was written through contributions of all authors. All authors have given approval to the final version of the manuscript.

Notes

The authors declare no competing financial interest.

■ ACKNOWLEDGMENTS

The authors acknowledge the Swedish Research Council for Environment, Agricultural Sciences and Spatial Planning (Formas, 2015-01032) for financial support and thank Tamara Church for helpful input and linguistic revision of the manuscript.

■ REFERENCES

(1) Flieger, M.; Kantorova, M.; Prell, A.; Rezanka, T.; Votruba, J. Biodegradable Plastics from Renewable Sources. *Folia Microbiol. (Dordrecht, Neth.)* **2003**, *48* (1), 27.

(2) Klemm, D.; Kramer, F.; Moritz, S.; Lindström, T.; Ankerfors, M.; Gray, D.; Dorris, A. Nanocelluloses: A New Family of Nature-Based Materials. *Angew. Chem., Int. Ed.* **2011**, *50* (24), 5438−5466.

(3) Spence, K. L.; Venditti, R. A.; Rojas, O. J.; Habibi, Y.; Pawlak, J. J. A Comparative Study of Energy Consumption and Physical Properties of Microfibrillated Cellulose Produced by Different Processing Methods. *Cellulose* **2011**, *18* (4), 1097−1111.

(4) Abitbol, T.; Rivkin, A.; Cao, Y.; Nevo, Y.; Abraham, E.; Ben-Shalom, T.; Lapidot, S.; Shoseyov, O. Nanocellulose, a Tiny Fiber with Huge Applications. *Curr. Opin. Biotechnol.* **2016**, *39*, 76−88.

(5) Dufresne, A. Nanocellulose: A New Ageless Bionanomaterial. *Mater. Today* **2013**, *16* (6), 220−227.

(6) Benítez, A. J.; Torres-Rendon, J.; Poutanen, M.; Walther, A. Humidity and Multiscale Structure Govern Mechanical Properties and Deformation Modes in Films of Native Cellulose Nanofibrils. *Biomacromolecules* **2013**, *14* (12), 4497−4506.

(7) Dunlop-Jones, N. Wet-Strength Chemistry. In *Paper Chemistry*; Springer, 1991; pp 76−96.

(8) Henschen, J.; Larsson, P. A.; Illergård, J.; Ek, M.; Wågberg, L. Bacterial Adhesion to Polyvinylamine-Modified Nanocellulose Films. *Colloids Surf., B* **2017**, *151*, 224−231.

(9) Larsson, P. A.; Berglund, L. A.; Wågberg, L. Highly Ductile Fibres and Sheets by Core-Shell Structuring of the Cellulose Nanofibrils. *Cellulose* **2014**, *21* (1), 323−333.

(10) Spoljaric, S.; Salminen, A.; Luong, N. D.; Seppälä, J. Crosslinked Nanofibrillated Cellulose: Poly(Acrylic Acid) Nanocomposite Films; Enhanced Mechanical Performance in Aqueous Environments. *Cellulose* **2013**, *20* (6), 2991−3005.

(11) Yang, W.; Bian, H.; Jiao, L.; Wu, W.; Deng, Y.; Dai, H. High Wet-Strength, Thermally Stable and Transparent TEMPO-Oxidized Cellulose Nanofibril Film: Via Cross-Linking with Poly-Amide Epichlorohydrin Resin. *RSC Adv.* **2017**, *7* (50), 31567−31573.

(12) Lossada, F.; Guo, J.; Jiao, D.; Groeer, S.; Bourgeat-Lami, E.; Montarnal, D.; Walther, A. Vitrimer Chemistry Meets Cellulose Nanofibrils: Bioinspired Nanopapers with High Water Resistance and Strong Adhesion. *Biomacromolecules* **2019**, *20* (2), 1045−1055.

(13) Hoenders, D.; Guo, J.; Goldmann, A. S.; Barner-Kowollik, C.; Walther, A. Photochemical Ligation Meets Nanocellulose: A Versatile Platform for Self-Reporting Functional Materials. *Mater. Horiz.* **2018**, *5* (3), 560−568.

(14) Sethi, J.; Visanko, M.; Österberg, M.; Sirviö, J. A. A Fast Method to Prepare Mechanically Strong and Water Resistant Lignocellulosic Nanopapers. *Carbohydr. Polym.* **2019**, *203*, 148−156.

(15) Wang, Q.; Du, H.; Zhang, F.; Zhang, Y.; Wu, M.; Yu, G.; Liu, C.; Li, B.; Peng, H. Flexible Cellulose Nanopaper with High Wet Tensile Strength, High Toughness and Tunable Ultraviolet Blocking Ability Fabricated from Tobacco Stalk via a Sustainable Method. *J. Mater. Chem. A* **2018**, *6*, 13021.

(16) Shimizu, M.; Saito, T.; Isogai, A. Water-Resistant and High Oxygen-Barrier Nanocellulose Films with Interfibrillar Cross-Linkages Formed through Multivalent Metal Ions. *J. Membr. Sci.* **2016**, *500*, 1−7.

(17) Toivonen, M. S.; Kurki-Suonio, S.; Schacher, F. H.; Hietala, S.; Rojas, O. J.; Ikkala, O. Water-Resistant, Transparent Hybrid Nanopaper by Physical Cross-Linking with Chitosan. *Biomacromolecules* **2015**, *16* (3), 1062−1071.

(18) Pahimanolis, N.; Salminen, A.; Penttilä, P. A.; Korhonen, J. T.; Johansson, L. S.; Ruokolainen, J.; Serimaa, R.; Seppälä, J. Nanofibrillated Cellulose/Carboxymethyl Cellulose Composite with Improved Wet Strength. *Cellulose* **2013**, *20* (3), 1459−1468.

(19) Benselfelt, T.; Engström, J.; Wagberg, L. Supramolecular Double Networks of Cellulose Nanofibrils and Algae Polysaccharides with Excellent Wet Mechanical Properties. *Green Chem.* **2018**, *20* (11), 2558−2570.

(20) Benselfelt, T.; Nordenström, M.; Lindström, S. B.; Wågberg, L. Explaining the Exceptional Wet Integrity of Transparent Cellulose Nanofibril Films in the Presence of Multivalent Ions—Suitable Substrates for Biointerfaces. *Adv. Mater. Interfaces* **2019**, *6*, 1−10.

(21) Gómez-Estaca, J.; López-de-Dicastillo, C.; Hernández-Muñoz, P.; Catalá, R.; Gavara, R. Advances in Antioxidant Active Food Packaging. *Trends Food Sci. Technol.* **2014**, *35* (1), 42−51.

(22) Bideau, B.; Bras, J.; Adoui, N.; Loranger, E.; Daneault, C. Polypyrrole/Nanocellulose Composite for Food Preservation: Barrier and Antioxidant Characterization. *Food Packag. Shelf Life* **2017**, *12*, 1−8.

(23) Ataide, J. A.; De Carvalho, N. M.; Rebelo, M. D. A.; Chaud, M. V.; Grotto, D.; Gerenutti, M.; Rai, M.; Mazzola, P. G.; Jozala, A. F. Bacterial Nanocellulose Loaded with Bromelain: Assessment of Antimicrobial, Antioxidant and Physical-Chemical Properties. *Sci. Rep.* **2017**, *7* (1), 2−10.

(24) dos Santos, C. A.; dos Santos, G. R.; Soeiro, V. S.; dos Santos, J. R.; Rebelo, M. de A.; Chaud, M. V.; Gerenutti, M.; Grotto, D.; Pandit, R.; Rai, M.; Jozala, A. F. Bacterial Nanocellulose Membranes Combined with Nisin: A Strategy to Prevent Microbial Growth. *Cellulose* **2018**, *25* (11), 6681−6689.
(25) Alzate-Arbeláez, A. F.; Dorta, E.; López-Alarcón, C.; Cortés, F. B.; Rojano, B. A. Immobilization of Andean Berry (Vaccinium Meridionale) Polyphenols on Nanocellulose Isolated from Banana Residues: A Natural Food Additive with Antioxidant Properties. *Food Chem.* **2019**, *294*, 503−517.
(26) Valencia, L.; Nomena, E. M.; Mathew, A. P.; Velikov, K. P. Biobased Cellulose Nanofibril-Oil Composite Films for Active Edible Barriers. *ACS Appl. Mater. Interfaces* **2019**, *11* (17), 16040−16047.
(27) Missio, A. L.; Mattos, B. D.; Ferreira, D. de F.; Magalhães, W. L. E.; Bertuol, D. A.; Gatto, D. A.; Petutschnigg, A.; Tondi, G. Nanocellulose-Tannin Films: From Trees to Sustainable Active Packaging. *J. Cleaner Prod.* **2018**, *184*, 143−151.
(28) Li, P.; Sirviö, J. A.; Haapala, A.; Khakalo, A.; Liimatainen, H. Anti-Oxidative and UV-Absorbing Biohybrid Film of Cellulose Nanofibrils and Tannin Extract. *Food Hydrocolloids* **2019**, *92*, 208−2017.
(29) Limaye, M. V.; Schütz, C.; Kriechbaum, K.; Wohlert, J.; Bacsik, Z.; Wohlert, M.; Xia, W.; Pléa, M.; Dembele, C.; Salazar-Alvarez, G.; Bergström, L. Functionalization and Patterning of Nanocellulose Films by Surface-Bound Nanoparticles of Hydrolyzable Tannins and Multivalent Metal Ions. *Nanoscale* **2019**, *11* (41), 19278−19284.
(30) Hagerman, A. E.; Butler, L. G. The Specificity of Proanthocyanidin-Protein Interactions. *J. Biol. Chem.* **1981**, *256* (9), 4494−4497.
(31) Covington, A. D. Modern Tanning Chemistry. *Chem. Soc. Rev.* **1997**, *26* (2), 111−126.
(32) Kriechbaum, K.; Munier, P.; Apostolopoulou-Kalkavoura, V.; Lavoine, N. Analysis of the Porous Architecture and Properties of Anisotropic Nanocellulose Foams - A Novel Approach to Assess the Quality of Cellulose Nanofibrils (CNFs). *ACS Sustainable Chem. Eng.* **2018**, *6*, 11959−11967.
(33) Head, F. S. H.; Standing, H. A. Reactions in Aqueous Solutions of Sodium Metaperiodate Exposed to Artificial Light. *J. Chem. Soc.* **1952**, *0*, 1457−1460.
(34) Zhao, H.; Heindel, N. D. Determination of Degree of Substitution of Formyl Groups in Polyaldehyde Dextran by the Hydroxylamine Hydrochloride Method. *Pharm. Res.* **1991**, *8* (3), 400−402.
(35) Dash, R.; Foston, M.; Ragauskas, A. J. Improving the Mechanical and Thermal Properties of Gelatin Hydrogels Cross-Linked by Cellulose Nanowhiskers. *Carbohydr. Polym.* **2013**, *91* (2), 638−645.
(36) Stryer, L. *Biochemistry*, 3rd ed.; Freeman, 1988.
(37) Bondet, V.; Brand-Williams, W.; Berset, C. Kinetics and Mechanisms of Antioxidant Activity Using the DPPH. Free Radical Method. *LWT-Food Sci. Technol.* **1997**, *30* (6), 609−615.
(38) Wang, Y.; Jiang, L.; Duan, J.; Shao, S. Effect of the Carbonyl Content on the Properties of Composite Films Based on Oxidized Starch and Gelatin. *J. Appl. Polym. Sci.* **2013**, *130* (5), 3809−3815.
(39) Painter, T. J. Control of Depolymerisation during the Preparation of Reduced Dialdehyde Cellulose. *Carbohydr. Res.* **1988**, *179* (C), 259−268.
(40) Kim, U.-J.; Kuga, S.; Wada, M.; Okano, T.; Kondo, T. Periodate Oxidation of Crystalline Cellulose. *Biomacromolecules* **2000**, *1* (3), 488−492.
(41) Nam, S.; Condon, B. D.; Xia, Z.; Nagarajan, R.; Hinchliffe, D. J.; Madison, C. A. Intumescent Flame-Retardant Cotton Produced by Tannic Acid and Sodium Hydroxide. *J. Anal. Appl. Pyrolysis* **2017**, *126*, 239−246.
(42) Hagerman, A. E. Fifty Years of Polyphenol − Protein Complexes. *Recent Adv. Polyphen. Res.* **2012**, *3*, 71−97.
(43) Le Bourvellec, C.; Renard, C. M. G. C. Interactions between Polyphenols and Macromolecules: Quantification Methods and Mechanisms. *Crit. Rev. Food Sci. Nutr.* **2012**, *52* (3), 213−248.
(44) Frazier, R. A.; Papadopoulou, A.; Mueller-Harvey, I.; Kissoon, D.; Green, R. J. Probing Protein-Tannin Interactions by Isothermal Titration Microcalorimetry. *J. Agric. Food Chem.* **2003**, *51* (18), 5189−5195.
(45) Saito, T.; Isogai, A. Introduction of Aldehyde Groups on Surfaces of Native Cellulose Fibers by TEMPO-Mediated Oxidation. *Colloids Surf., A* **2006**, *289* (1−3), 219−225.
(46) Quero, F.; Padilla, C.; Campos, V.; Luengo, J.; Caballero, L.; Melo, F.; Li, Q.; Eichhorn, S. J.; Enrione, J. Stress Transfer and Matrix-Cohesive Fracture Mechanism in Microfibrillated Cellulose-Gelatin Nanocomposite Films. *Carbohydr. Polym.* **2018**, *195*, 89−98.
(47) Sehaqui, H.; Ezekiel Mushi, N.; Morimune, S.; Salajkova, M.; Nishino, T.; Berglund, L. A. Cellulose Nanofiber Orientation in Nanopaper and Nanocomposites by Cold Drawing. *ACS Appl. Mater. Interfaces* **2012**, *4* (2), 1043−1049.
(48) Briassoulis, D.; Giannoulis, A. Evaluation of the Functionality of Bio-Based Food Packaging Films. *Polym. Test.* **2018**, *69*, 39−51.
(49) Oliveira, V. M.; Nogueira, B. R.; Ortiz, A. V.; Moura, E. A. B. Mechanical and Thermal Properties of Commercial Multilayer Flexible Plastic Packaging Materials Irradiated with Electron Beam. *Nukleonika* **2008**, *53*, 141−144.
(50) Vanstrom, J. R. Mechanical Characterization of Commercial Biodegradable Plastic Films. *Ph.D. Thesis*, Iowa State University, 2012; Vol. *12661*.
(51) Rennert, M.; Nase, M.; Lach, R.; Reincke, K.; Arndt, S.; Androsch, R.; Grellmann, W. Influence of Low-Density Polyethylene Blown Film Thickness on the Mechanical Properties and Fracture Toughness. *J. Plast. Film Sheeting* **2013**, *29* (4), 327−346.
(52) Rhim, J. W. Effect of Moisture Content on Tensile Properties of Paper-Based Food Packaging Materials. *Food Sci. Biotechnol.* **2010**, *19* (1), 243−247.
(53) Hagerman, A. E.; Butler, L. G. Protein Precipitation Method for the Quantitative Determination of Tannins. *J. Agric. Food Chem.* **1978**, *26* (4), 809−812.
(54) Widsten, P.; Cruz, C. D.; Fletcher, G. C.; Pajak, M. A.; McGhie, T. K. Tannins and Extracts of Fruit Byproducts: Antibacterial Activity against Foodborne Bacteria and Antioxidant Capacity. *J. Agric. Food Chem.* **2014**, *62* (46), 11146−11156.
(55) Glaive, A.-S.; Modjinou, T.; Versace, D.-L.; Abbad-Andaloussi, S.; Dubot, P.; Langlois, V.; Renard, E. Design of Antibacterial and Sustainable Antioxidant Networks Based on Plant Phenolic Derivatives Used as Delivery System of Carvacrol or Tannic Acid. *ACS Sustainable Chem. Eng.* **2017**, *5*, 2320.
(56) Quideau, S.; Deffieux, D.; Douat-Casassus, C.; Pouységu, L. Plant Polyphenols: Chemical Properties, Biological Activities, and Synthesis. *Angew. Chem., Int. Ed.* **2011**, *50* (3), 586−621.

https://dx.doi.org/10.1021/acs.biomac.9b01655
Biomacromolecules 2020, 21, 1720−1728